**Short Communication** 

© Hasegawa Y, et al. 2025

# Identification and Functional Analysis of a Novel *SLC12A3* Mutation in Japanese Gitelman Syndrome

Hiraku Chiba<sup>1</sup>, Yutaka Hasegawa<sup>1</sup>, Yuichiro Kezuka<sup>2,3</sup>, Ai Chida<sup>1</sup>, Eriko Yoshida<sup>1</sup>, Toshie Segawa<sup>1</sup>, Tomoyasu Oda<sup>1</sup>, Yoshihiko Takahashi<sup>1</sup>, Takuya Noguchi<sup>4</sup>, Koji Nata<sup>4</sup>, and Yasushi Ishigaki<sup>1</sup>

<sup>1</sup>Department of Internal Medicine, Iwate Medical University, Japan
<sup>2</sup>Thermo Fisher Scientific, Life Technologies Japan Ltd., Japan
<sup>3</sup>Department of Pharmaceutical Sciences, Iwate Medical University, Japan
<sup>4</sup>Division of Medical Biochemistry, School of Pharmacy, Iwate Medical University, Yahaba, Japan

#### **Abstract**

**Background :** Gitelman syndrome (GS) is a rare autosomal recessive disorder caused by mutations in the *SLC12A3* gene, which encodes the sodium-chloride (Na-Cl) cotransporter (NCC). GS is characterized by salt-losing tubulopathy, which leads to renal potassium loss, hypokalemia, metabolic alkalosis, hypocalciuria, hypomagnesemia, and hyperreninemic hyperaldosteronism. GS can increase the risk of developing type 2 diabetes mellitus.

**Case presentation:** We report the case of a Japanese patient with GS who had suffered from hypokalemia for over a decade, and subsequently developed diabetes. The results of detailed biochemistry and diuretic stress tests suggested a diagnosis of GS.

**Results :** Genetic exome sequencing revealed both heterozygous c.835A>G (p.Met279Val) and homozygous c.791C>G (p.Ala264Gly) mutations in the *SLC12A3* gene. Further in silico variant prediction and structural analyses revealed that the heterozygous c.835A>G (p.Met279Val) mutation in the *SLC12A3* gene was the predominant pathogenic variant. Modeling and structural analyses suggested that this mutation contributes to the NCC salt-bridge conformation and leads to impaired Na-Cl transport.

**Conclusion :** We present a case of GS with a novel *SLC12A3* gene mutation that has not been previously reported. Genetic testings and structural analyses are essential for the accurate diagnosis and understanding of the renal tubular pathology in GS.

Keywords: SLC12A3; Gitelman syndrome; Na-Cl cotransporter (NCC); Hypokalemia; Normomagnesemia

### **INTRODUCTION**

Gitelman syndrome (GS) is a recessive salt-wasting tubular disorder characterized by hypomagnesemia, hypokalemia, metabolic alkalosis, hypocalciuria, and activation of the renin-angiotensin-aldosterone (RAA) system [1]. GS is not a benign condition and often presents with nonspecific symptoms, such as muscle weakness, tetany, hypotension, and fatigue [2]. Other common symptoms include prolonged QTc interval and arrhythmias due to hypokalemia [3,4]. Additionally, GS has been reported as a risk factor for developing type 2 diabetes mellitus [5]. Factors contributing to this susceptibility include impaired insulin secretion due to chronic hypokalemia [6], and insulin resistance due to

Submitted: 17 August 2025 | Accepted: 19 September 2025 | Published: 19 September 2025

\*Corresponding author: Yutaka Hasegawa, Department of Internal Medicine, Iwate Medical University, 2-1-1 Idaidori, Yahaba, Iwate, 028-3695, Japan, Tel: 81-19-613-7111

**Copyright:** © 2025 Hasegawa Y, et al. This is an open-access article distributed under the terms of the Creative Commons Attribution License, which permits unrestricted use, distribution, and reproduction in any medium, provided the original author and source are credited.

Citation: Chiba H, Hasegawa Y, Kezuka Y, Chida A, Yoshida E, et al. (2025) Identification and Functional Analysis of a Novel *SLC12A3* Mutation in Japanese Gitelman Syndrome. J Nephrol Kidney Dis 6(2): 7.

hyperaldosteronism [7].

GS is caused by a mutation in the *SLC12A3* gene, which encodes the NCC that is highly expressed in the apical membrane of the distal convoluted tubule (DCT) [8,9]. Definitive diagnosis of tubular abnormalities, including GS, Bartter syndrome (BS), pseudo-BS, and pseudo-GS, is essential for appropriate clinical management [10].

We encountered a case of GS that was diagnosed by biochemical and diuretic loading tests and identified a novel *SLC12A3* gene mutation through genetic testing. Further *in silico* and structural analyses predicted the responsible *SLC12A3* gene mutation results in the dysfunction of NCC.

# **METHODS**

### **Ethics statement**

Written informed consent was obtained from the patient. All clinical investigations were conducted in accordance with the principles of the Declaration of Helsinki.

### **Genetic analysis**

Mutation analysis was performed in genes related to hereditary BS/GS (e.g., *SLC12A1, KCNJ1, CLCNKB, BSND, CLCNKA, MAGED2, CASR, SLC12A3, CFTR, EHD1, HNF1B, KCNJ10, KCNJ2, KCNJ5*, and *SLC26A3*), by a next-generation sequencer at the Kazusa DNA Laboratory.

# **Homology modeling**





Models of the p.Ala264Gly, p.Met279Val mutants of SLC12A3 were generated by the SWISS modelling server [11], on the basis of the crystal structure of human NCC [12,13]. Then, the models were energy-minimized using the minimization routines included in the UCSF Chimera program [14].

### **RESULTS**

### **Case presentation**

A 44-year-old Japanese woman presented with complaints of dry mouth, polydipsia, polyuria, fatigue, and weakness that had persisted for several months. She was diagnosed with diabetes based on a postprandial blood glucose level of 778 mg/dL and an HbA1c level of 19.9%, and was admitted to the previous hospital for treatment. Since autoantibodies associated with type 1 diabetes, such as anti-insulin, anti-glutamic acid decarboxylase (GAD), and anti-insulinoma-associated antigen 2 (IA-2) antibodies were negative, the patient was diagnosed with type 2 diabetes. She was discharged after switching from insulin to oral therapy. Following discharge, she was referred to our hospital for evaluation of longstanding, undiagnosed hypokalemia that had been persistent since her late 30s. Her medical history included depression, uterine myoma surgery in her late 30s, and ischemic enteritis at age 43. There was no family history of hypokalemia and type 2 diabetes.

 $Biochemical \ tests \ at \ the \ time \ of admission \ showed \ that \ the \ HbA1c \ level$ remained elevated at 15.7%, while fasting blood glucose was normal (93 mg/dL), and endogenous insulin secretion was preserved, with a fasting C-peptide immunoreactivity (CPR) of 3.18 ng/mL (Table 1). The patient exhibited hypokalemia (3.0 mEq/L), hypochloremia (93 mEq/L), and normomagnesemia (2.2 mg/dL) with oral potassium supplementation (30 mEq/day). The RAA system was activated without the administration of diuretics (Table 1). Venous blood gas analysis revealed alkalemia with a high pH (7.47) and elevated HCO<sub>3</sub> (34 mmol/L), indicating metabolic alkalosis (base excess: 9.2 mmol/L). There was no history of laxative overuse, diarrhea, or vomiting. The transtubular potassium gradient was elevated at 11.8. Due to suspected salt-losing tubulopathy, diuretic loading tests were conducted to evaluate renal tubular function [9,15]. Diuretic loading tests, which are designed to evaluate distal fractional chloride reabsorption (DFCR)-an index of distal tubular Cl<sup>-</sup> reabsorptiondemonstrated contrasting responses (Table 2). DFCR decreased markedly after furosemide loading but remained unchanged following thiazide load. These findings indicated a blunted response of the thiazide-sensitive NCC, which was consistent with GS.

The patient's serum potassium levels improved with supplementation. Since then, her glycemic control has stabilized, with HbA1c improving to approximately 6% alongside the correction of hypokalemia.

# Identification of a novel missense *SLC12A3* gene mutation by exome sequencing

After obtaining written informed consent from the patient, we performed genetic analysis using direct sequencing. Whole-exome sequencing of the *SLC12A3* gene revealed one homozygous missense mutation (c.791C>G, p.Ala264Gly) and one heterozygous missense mutation (c.835A>G, p.Met279Val) (Figure 1A). Previous reports have revealed that the p.Ala264Gly variant is not pathogenic, while others have described it as pathogenic [16], making its clinical significance controversial. However, *in silico* analysis of using PolyPhen-2 (http://genetics.bwh.harvard.edu/pph2/), MutationTaster (https://www.mutationtaster.org/), and Mendelian Clinically Applicable Pathogenicity

(M-CAP) [17], showed that this mutation was benign. In addition, its minor allele frequency (MAF) was relatively high (Figure 1A). Further alignment analysis of this residue revealed that the p.Ala264Gly variant is conserved among non-human animal genomes, including monkeys, rats, mice, chickens and frogs (Figure 1B), suggesting this variant does not contribute to major structural changes in SLC12A3 nor affect its function. In contrast, the p.Met279Val variant is a novel missense mutation that has not been previously reported. *In silico* analysis predicted that the p.Met279Val variant is probably damaging, with a PolyPhen-2 score of 0.904 and a pathogenic classification by M-CAP. Furthermore, this region is conserved across multiple species and is, therefore, considered a functionally critical region (Figure 1B).

# Structural analysis of p.Ala264Gly and p.Met279Val variants in SLC12A3.

To investigate and predict the functional impact of these two variants, we performed modeling and structural analyses. Of the 12 transmembrane (TM) helices of SLC12A3, p.Ala264Gly is located in TM4, while p.Met279Val is located in the loop between TM4 and TM5 (Figure 1C). The effect of the p.Ala264Gly mutation in SLC12A3 is difficult to conclude because it is an amino acid substitution between two non-polar, neutral amino acids and because the sequence is conserved in animal species other than humans (Figure 1B). A previous report found that the Glu282 residue, which is structurally close to Met279, contributes to the outward-open conformation by forming a salt bridge with the Arg145 residue, as observed in the SLC12A3 structure (Figure 1D) [13]. Site-directed mutagenesis of Glu282 or Arg145 has been shown to severely impair transport activity and has been associated with GS [13]. The p.Met279Val mutation found in this patient, and positioned near the Glu282, likely caused a structural change that affects ion transport. Therefore, it can be suggested that the p.Met279Val mutation is the primary causative mutation in this case of GS.

### **DISCUSSION**

In this case, GS was diagnosed along with poorly controlled diabetes mellitus based on biochemical findings, including electrolyte abnormalities, metabolic alkalosis, and hyperreninemic hyperaldosteronism, and a blunted response to thiazide-sensitive NCC during diuretic loading tests. Additional genetic testing confirmed the definitive diagnosis of GS by identifying a novel causative *SLC12A3* gene mutation. Both BS and GS are genetic salt-losing tubulopathies characterized by hypokalemia, hyperreninemia-hyperaldosteronemia, and metabolic alkalosis. However, their treatment strategies differ. The diuretic loading tests are useful for differential diagnosis and for evaluating renal tubular function. Further genetic and structural analyses allowed for a detailed functional assessment of SLC12A3.

The two mutations identified in this patient were positioned relatively close to each other within the *SLC12A3* gene sequence and may jointly influence the function of *SLC12A3*. The p.Ala264Gly mutation in *SLC12A3* gene has previously been reported as both benign and pathogenic, making its clinical significance uncertain. In contrast, the p.Met279Val mutation in *SLC12A3* has not been previously reported and was predicted to be pathogenic based on *in silico* analyses. This mutation is located in the loop between TM4 and TM5, adjacent to Glu282. In the complex structure of *SLC12A3* and polythiazide, Glu282 and Arg145 formed a salt bridge that contributed to the outward-open conformation (Figure 1D). Additionally, the substitution of Arg145 or Glu282 with Ala significantly reduced transport activity and is therefore considered a mechanistic cause of GS



Table 1: Summary of laboratory data

	Component	Result	Reference range	
	TP (g/dL)	6.7	6.6-8.1	
	Albumin (g/dL)	4	4.1-5.1	
	Na (mEq/L)	139	138-145	
	K (mEq/L)	3	3.6-4.8	
	Cl (mEq/L)	93	101-108	
	Ca (mg/dL)	9.8	8.8-10.1	
	P (mg/dL)	4.3	2.7-4.6	
	Mg (mg/dL)	2.2	1.8-2.3	
	AST (U/L)	17	13-30	
	ALT (U/L)	13	7-23	
	LDH (U/L)	138	124-222	
	ALP (U/L)	71	38-113	
	γGTP (U/L)	21	9-32	
	T-Bil (mg/dL)	0.6	0.4-1.5	
	CK (U/L)	27	41-153	
	BUN (mg/dL)	17.5	8-20	
	Cr (mg/dL)	0.86	0.46-0.79	
Biochemistry	eGFR (mL/min/1.73m <sup>2</sup> )	56.7	>90	
Dioenemistry	UA (mg/dL)	8.1	2.6-5.5	
	T-chol (mg/dL)	258	142-248	
	TG (mg/dL)	268	30-117	
	Glucose (mg/dL)	93	73-109	
	HbA1c (%)	15.7	4.9-6.0	
	C-peptide (ng/mL)	3.18	0.5-2.0	
	Anti-GAD (U/mL)	<5.0	<5.0	
	Anti-IA-2 (U/mL)	<0.6	0-0.6	
	PAC (pg/mL)	200	4.0-82.1	
	PRA (ng/mL/h)	20.4	0.2-2.3	
	ACTH 8am (pg/mL)	13.9	7.2-63.3	
	Cortisol 8am (µg/dL)	8.3	7.07-19.6	
	TSH (μIU/mL)	3.03	0.5-5	
	Free T4 (ng/dL)	1.47	0.9-1.7	
	Free T3 (pg/mL)	2.91	2.3-4	



Blood count	WBC (×10³/μL)	7.69	3.3-8.6	
	RBC (×106/μL)	4.79	4.35-5.55	
	Hb (g/dL)	13.4	13.7-16.8	
	Ht (%)	41	40.7-50.1	
	PLT (×10³/μL)	439	158-348	
Venous blood gas analysis	рН	7.47	7.35-7.45	
	HCO <sub>3</sub> · (mmol/L)	34	22-26	
	BE (mmol/L)	9.2	-2-2	
Urine	Protein	-		
	Glucose	-		
orme	RBC	-		
	Ketone -			
Urine biochemistry	Na (mEq/g Cr)	3.89		
	K (mEq/g Cr)	29.5		
	Cl (mEq/g Cr)	6.2		
	Ca (mg/g Cr)	10.1		
	U <sub>osm</sub> (m0sm/kg H <sub>2</sub> 0)	344		
	FE <sub>Na</sub> (%)	0.02		
	FE <sub>K</sub> (%)	8.45		
	FE <sub>Cl</sub> (%)	0.01		
	24h urine volume (mL)	1400		

The results in bold are outside the limits of the normal value.

Abbreviations: TP: Total Protein; Na: Sodium; K: Potassium; Cl: Chloride; Ca: Calcium; P: Phosphate; Mg: Magnesium; AST: Aspartate Aminotransferase; ALT: Alanine Aminotransferase; LDH: Lactate Dehydrogenase; ALP: Alkaline Phosphatase;  $\gamma$ GTP: Gamma-Glutamyl Transpeptidase; T-Bil: Total Bilirubin; CK: Creatine Kinase; BUN: Blood Urea Nitrogen; Cr: Creatinine; eGFR: Estimated Glomerular Filtration Rate; UA: Uric Acid; T-chol: Total Cholesterol; TG: Triglyceride; HbA1c: Glycated Hemoglobin; Anti-GAD: Glutamic acid Decarboxylase Antibody; Anti-IA-2: Insulinoma-associated Antigen 2 Antibody; PAC: Plasma Aldosterone Concentration; PRA: Plasma Renin Activity; ACTH: Adrenocorticotropic Hormone; TSH: Thyroid Stimulating Hormone; WBC: White Blood Cells; RBC: Red Blood Cells; Hb: Hemoglobin; Ht: Hematocrit; MCV: Mean Corpuscular Volume; MCH: Mean Corpuscular Hemoglobin; MCHC: Mean Corpuscular Hemoglobin; MCHC: Mean Corpuscular Urine Osmolality; FE $_{\rm M}$ : Fractional Excretion of Sodium; FE $_{\rm K}$ : Fractional Excretion of Potassium; FE $_{\rm C}$ : Fractional Excretion of Chloride



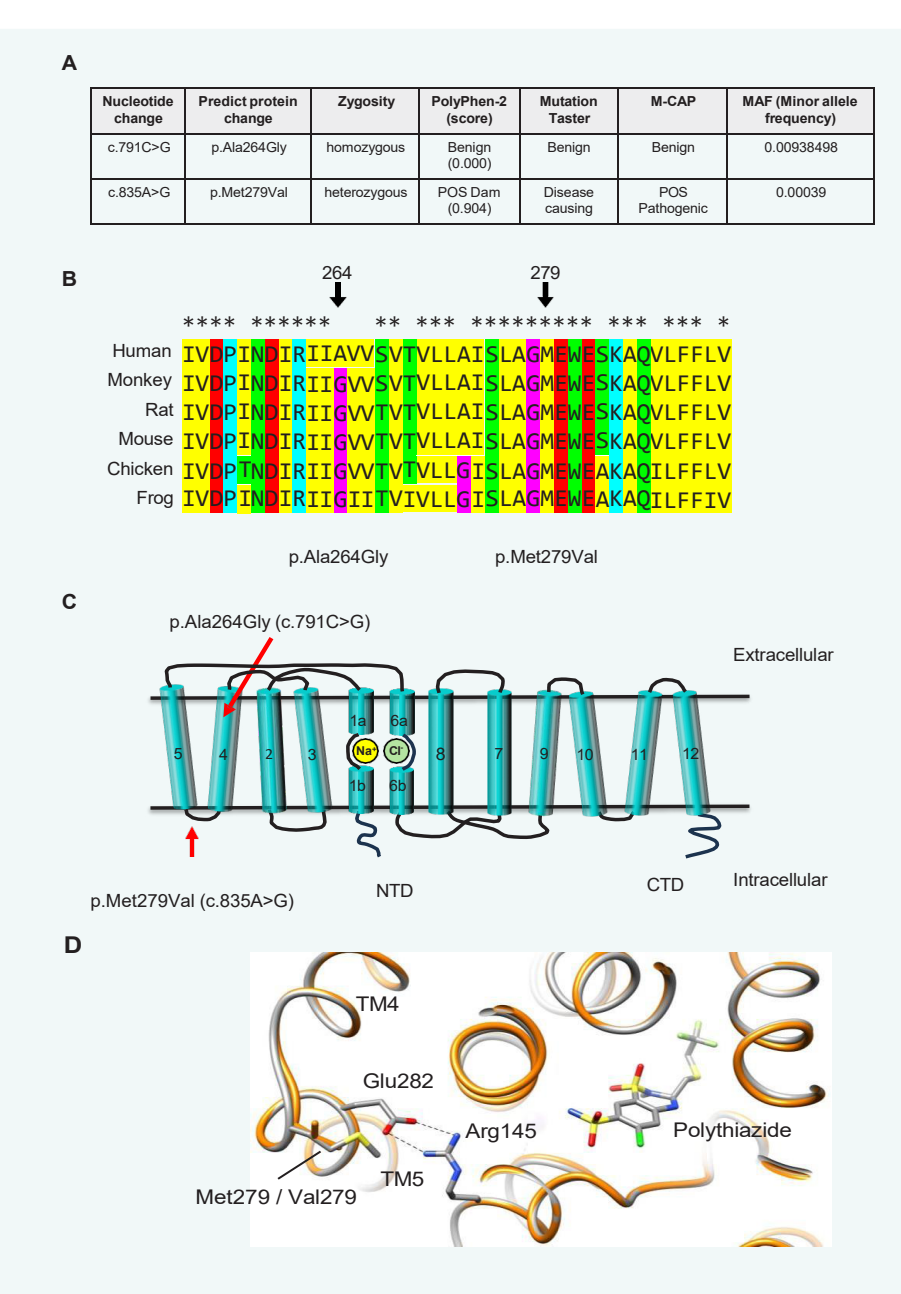


Figure 1: In silico and structural analysis of SLC12A3 mutants

(A) *In silico* analysis of the *SLC12A3* gene variants identified in this patient. (B) Evolutionarily conserved amino acid sequences surrounding the p.Ala264Gly and p.Met279Val mutation positions. The identification numbers of the *SLC12A3* nucleotides are as follows: Human (NP\_001126108.2), Monkey (XM\_074027036.1), Rat (XM\_032887934.1), Mouse (NM\_001205311.1), Chicken (XM\_040680995.2), Frog (XM\_002937171.5). The asterisk (\*) indicates the conserved residue. (C) Topology arrangement of SLC12A3. The protein is predicted to span the plasma membrane 12 times, with each transmembrane helix (TM1-TM12) shown as a light blue cylinder. TM1 and TM6 contain discontinuities in the middle of the helix, which are suitable for ion binding. The Na<sup>+</sup> and Cl<sup>-</sup> ions are depicted in yellow and green, respectively. The extracellular and intracellular orientations are indicated, and the N-terminal domain (NTD), and C-terminal domain (CTD), are shown as flexible loops. Red arrows highlight the two missense variants identified in this study: c.791C>G (p.Ala264Gly), located within TM4, and c.835A>G (p.Met279Val), located in the loop between TM4 and TM5. (D) Overlay of the wild-type SLC12A3 in the outward-open conformation and the Ala264Gly/Met279Val mutant model (orange). The p.Met279Val mutation site, Glu282, Arg145, and a bound polythiazide molecule are shown. A salt bridge between Glu282 and Arg145 is illustrated with dashed lines.



### Table 2: Summary of diuretic loading tests

The furosemide (20 mg, intravenously) and thiazide (50 mg, orally) loading tests were performed on separate days.

DFCR=
$$C_{H_{2}O}$$
 /  $(C_{H_{2}O} + C_{Cl})$ ,  $C_{H_{2}O}$  =  $(1-U_{osm}/P_{osm}) \times V$ ,  $C_{Cl}$  =  $U_{Cl} \times V / P_{Cl}$ 

Pre loading: Measurements obtained before the furosemide or thiazide load.

Post loading: Measurements obtained at the time of peak urine flow rate after the furosemide or thiazide load.

Furosemide (20 mg)	V (mL/20 min)	U <sub>osm</sub> (m0sm/kg H <sub>2</sub> 0)	P <sub>osm</sub> (mOsm/kg H <sub>0</sub> 0)	C <sub>H2O</sub> (mL/20 min)	U <sub>cı</sub> (mEq/L)	P <sub>Cl</sub>	C <sub>CI</sub> (mL/20 min)	DFCR (%)
Pre loading	60	92	268	39.4	8	89	5.4	88
Post loading	364	144	269	169.1	49	90	198.1	46.1
Thiazide (50 mg)	V (mL/30 min)	U <sub>osm</sub> (m0sm/kg H <sub>2</sub> 0)	P <sub>osm</sub> (mOsm/kg H <sub>2</sub> O)	C <sub>H2O</sub> (mL/30 min)	U <sub>cı</sub> (mEq/L)	P <sub>Cl</sub>	C <sub>CI</sub> (mL/30 min)	DFCR (%)
Pre loading	82	62	266	58.5	7	90	6.4	90.2
Post loading	112	82	269	77.9	12	92	14.6	84.2

Abbreviations: DFCR: Distal Fractional Chloride Reabsorption;  $C_{H_2O}$ : Solute Free Water Clearance;  $C_{Cl}$ : Chloride Clearance; V: Volume of Urine Flow Rate;  $U_{osm}$ : Urinary Osmolality,  $P_{osm}$ : Plasma Osmolality;  $U_{Cl}$ : Urinary Chloride,  $P_{Cl}$ : Plasma Chloride

[13]. Another report revealed that the p.Met279Arg mutation at the same position identified in our patient, was causative of GS through a similar mechanism [16].

Although most cases of GS are recessive genetic disorders caused by biallelic mutations, several cases involving dominant mutations have been reported, including Gitelman-like syndrome [18]. In addition, large genomic rearrangements can cause GS and have been detected in approximately half of patients with a heterozygous *SLC12A3* gene mutation [18]. Since we did not perform a genomic rearrangement analysis, we cannot exclude the possibility that such a genomic rearrangement occurred in this case.

This patient was hospitalized due to poorly controlled diabetes mellitus, which may have been influenced by reduced physical activity and excessive carbohydrate intake during the COVID-19 pandemic. Additional contributing factors included hypokalemia and insulin resistance caused by GS. Indeed, glycemic control has been stabilized following improvements in GS-related pathology, including hypokalemia, metabolic alkalosis, hypocalciuria, and activation of the RAA system.

### **CONCLUSION**

We experienced a case of Gitelman syndrome by identifying a novel heterozygous *SLC12A3* gene mutation (c.835A>G, p.Met279Val) and a homozygous *SLC12A3* gene mutation (c.791C>G, p.Ala264Gly). Further *in silico* analysis revealed that the p.Met279Val mutation is the primary causative gene mutation in this GS patient.

### **FUNDING**

This research did not receive any specific grants from funding agencies in the public, commercial, or nonprofit sectors.

# **ACKNOWLEDGEMENTS**

The authors thank the patient for consenting to the publication of this case report. They also express their gratitude to Dr. Minoru Kawamura for his role in the initial management of the patient.

### **AUTHORS' CONTRIBUTIONS**

Chiba H and Hasegawa Y collected the patient data, performed the in silico analyses, and drafted the manuscript. Kezuka Y performed the structural analysis. Segawa T, Chida A, Chiba H, Oda T and Takahashi Y were involved in the clinical management of the patient. Nata K and Noguchi T contributed to the data analysis. Ishigaki Y reviewed and revised the manuscript. All the authors have read and approved the final version of the manuscript.

# **REFERENCES**

- Knoers NV, Levtchenko EN. Gitelman syndrome. Orphanet J Rare Dis. 2008; 3: 22.
- Schlingmann KP, de Baaij JHF. The genetic spectrum of Gitelman(-like) syndromes. Curr Opin Nephrol Hypertens 2022; 31: 508-515.
- 3. Courand PY, Marques P, Vargas-Poussou R, Azizi M, Blanchard A, investigators Gs. QT Interval in Adult with Chronic Hypokalemia due to Gitelman Syndrome: Not so Frequently Prolonged. Clin J Am Soc Nephrol. 2020; 15: 1640-1642.
- Pachulski RT, Lopez F, Sharaf R. Gitelman's not-so-benign syndrome. N Engl J Med. 2005; 353: 850-851.
- Yuan T, Jiang L, Chen C, Peng X, Nie M, Li X, et al. Glucose tolerance and insulin responsiveness in Gitelman syndrome patients. Endocr Connect. 2017; 6: 243-252.
- Shafi T, Appel LJ, Miller ER 3rd, Klag MJ, Parekh RS. Changes in serum potassium mediate thiazide-induced diabetes. Hypertension. 2008; 52: 1022-1029.
- Reincke M, Meisinger C, Holle R, Quinkler M, Hahner S, Beuschlein F, et al. Participants of the German Conn's R: Is primary aldosteronism associated with diabetes mellitus? Results of the German Conn's Registry. Horm Metab Res. 2010; 42: 435-439.





- 8. Simon DB, Nelson-Williams C, Bia MJ, Ellison D, Karet FE, Molina AM, et al. Gitelman's variant of Bartter's syndrome, inherited hypokalaemic alkalosis, is caused by mutations in the thiazide-sensitive Na-Cl cotransporter. Nat Genet. 1996; 12: 24-30.
- Colussi G, Bettinelli A, Tedeschi S, De Ferrari ME, Syren ML, Borsa N, et al. A thiazide test for the diagnosis of renal tubular hypokalemic disorders. Clin J Am Soc Nephrol. 2007; 2: 454-460.
- Matsunoshita N, Nozu K, Shono A, Nozu Y, Fu XJ, Morisada N, et al. Differential diagnosis of Barttersyndrome, Gitelman syndrome, and pseudo-Bartter/Gitelman syndrome based on clinical characteristics. Genet Med. 2016; 18: 180-188.
- Schwede T, Kopp J, Guex N, Peitsch MC. SWISS-MODEL: An automated protein homology-modeling server. Nucleic Acids Res. 2003; 31: 3381-3385
- Nan J, Yuan Y, Yang X, Shan Z, Liu H, Wei F, et al. Cryo-EM structure of the human sodium-chloride cotransporter NCC. Sci Adv. 2022; 8: eadd7176.
- Fan M, Zhang J, Lee CL, Zhang J, Feng L. Structure and thiazide inhibition mechanism of the human Na-Cl cotransporter. Nature. 2023; 614: 788-793.

- 14. Pettersen EF, Goddard TD, Huang CC, Couch GS, Greenblatt DM, Meng EC, et al. UCSF Chimera--a visualization system for exploratory research and analysis. J Comput Chem. 2004; 25: 1605-1612.
- Tsukamoto T, Kobayashi T, Kawamoto K, Fukase M, Chihara K. Possible discrimination of Gitelman's syndrome from Bartter's syndrome by renal clearance study: report of two cases. Am J Kidney Dis. 1995; 25: 637-641.
- Portioli C, Ruiz Munevar MJ, De Vivo M, Cancedda L. Cation-coupled chloride cotransporters: chemical insights and disease implications. Trends Chem. 2021; 3: 832-849.
- Jagadeesh KA, Wenger AM, Berger MJ, Guturu H, Stenson PD, Cooper DN, et al. M-CAP eliminates a majority of variants of uncertain significance in clinical exomes at high sensitivity. Nat Genet. 2016; 48: 1581-1586.
- Vargas-Poussou R, Dahan K, Kahila D, Venisse A, Riveira-Munoz E, Debaix H, et al. Spectrum of mutations in Gitelman syndrome. J Am Soc Nephrol. 2011; 22: 693-703.